

## Article

# Electromagnetic Shielding of Composite Films Based on Graphite, Graphitized Carbon Black and Iron-Oxide

Volodymyr Khomenko <sup>1,\*</sup>, Oksana Butenko <sup>1</sup>, Oksana Chernysh <sup>1</sup>, Viacheslav Barsukov <sup>1</sup> ,  
Mirela Petruta Sucheai <sup>2,3,\*</sup>  and Emmanouel Koudoumas <sup>2</sup>

<sup>1</sup> Kyiv National University of Technologies and Design, 2 Nemyrovych-Danchenko Str., 01011 Kyiv, Ukraine; butenko.oo@knutd.edu.ua (O.B.); zaya1566@ukr.net (O.C.); v-barsukov@i.ua (V.B.)

<sup>2</sup> Center of Materials Technology and Photonic, Department of Electrical and Computer Engineering, Hellenic Mediterranean University, 71410 Heraklion, Greece; koudoumas@hmu.gr

<sup>3</sup> National Institute for Research and Development in Microtechnologies (IMT-Bucharest), 023573 Bucharest, Romania

\* Correspondence: v.khomenko@i.ua (V.K.); mirasuchea@hmu.gr or mira.suchea@imt.ro (M.P.S.); Tel.: +380-98-849-85-17 (V.K.)

**Abstract:** The present work regards the development of paint-like composites based on mixtures of carbon materials with magnetite in polyvinyl butyral matrix, and the investigation of the dependence on the electrical characteristics and the frequency of their electromagnetic shielding properties. It was found that high electromagnetic shielding effectiveness requires not only the presence of a high content of carbon components in the composite, but also the absence of an agglomeration of filler particles. Using these paint-like materials, a shielding effectiveness of up to  $-35$  dB of UHF radiation can be obtained. A combination of fillers based on carbon-graphite materials of different morphology and magnetite was found to enhance shielding efficiency.

**Keywords:** polymer composites; electromagnetic interference shielding; carbon composites



**Citation:** Khomenko, V.; Butenko, O.; Chernysh, O.; Barsukov, V.; Sucheai, M.P.; Koudoumas, E. Electromagnetic Shielding of Composite Films Based on Graphite, Graphitized Carbon Black and Iron-Oxide. *Coatings* **2022**, *12*, 665. <https://doi.org/10.3390/coatings12050665>

Academic Editor: Jiri Militky

Received: 30 April 2022

Accepted: 11 May 2022

Published: 13 May 2022

**Publisher's Note:** MDPI stays neutral with regard to jurisdictional claims in published maps and institutional affiliations.



**Copyright:** © 2022 by the authors. Licensee MDPI, Basel, Switzerland. This article is an open access article distributed under the terms and conditions of the Creative Commons Attribution (CC BY) license (<https://creativecommons.org/licenses/by/4.0/>).

## 1. Introduction

Today, electromagnetic radiation (EMR) has become a serious problem, as the use of electrical and electronic devices in our everyday life has greatly proliferated [1,2]. As a result, humans are surrounded by electromagnetic fields of different frequencies and strengths, and the respective hazards are widely discussed in the literature [3–5]. Experiments carried out by leading research institutions have shown that man-made electromagnetic fields, which are hundreds of times weaker than those of the Earth's natural field, can be hazardous to health. As an example, high-frequency radiation can ionize atoms and molecules in somatic cells and interfere with biochemical processes within the cells [6]. Moreover, EMR is capable of heating molecules and setting them into thermal motion [7]. Then, to reduce the impact of EMR on people exposed to it, it is necessary to take certain safety measures. Therefore, the development of protective methods and means for decreasing the intensity of EMR is important. To this aim, the use of composite electromagnetic screens and coatings is essential.

Another problem related to EMR shielding is the electromagnetic compatibility of devices, an issue that has been given much attention worldwide [7–9]. The problem refers to the stable operation of communication devices, hardware, etc., as their mutual effect might cause unstable performance. Bearing in mind this effect, a reduction in the electromagnetic field and increase in the electromagnetic compatibility can be achieved using electromagnetic shields [10,11]. Such shields can be prepared with metals (iron, steel, copper, brass, and aluminum) or polymer composites containing conductive additives [12,13], with the latter applied as thin films [14]. Today, EMI shielding materials include flexible metal screens, metal wires, and metal foams. Coatings made

of metallic inks are also applied to the interiors of electronic enclosures to provide an EMI shielding solution. Metals are distinguished by having a high reflection coefficient. However, metal shields have drawbacks [15] related to reflection, since they reradiate waves, which can enhance the exposure to radiation. Each of these shielding methods has its advantages, but lightweight paint-like carbon-based coatings combine the electrical properties of metal with excellent mechanical material properties at a lower cost and with easier application.

In this work, a polymer-carbon material is proposed that can provide high shielding coefficients, owing to a considerable absorption of EMR.

## 2. Materials and Methods

The aim of this work was to substantiate the possibility of using available and inexpensive carbon materials as components of EMR absorbents. Carbon-graphite materials of different morphology were examined, such as colloidal graphite CGP S-1 (Zavalivskiy Graphite, Kyiv, Ukraine) and graphitized carbon black «PUREBLACK®» (Superior Graphite Co. Chicago, Illinois, USA) in polyvinyl butyral PVB (Sigma, Taufkirchen, Germany). Pure ultrafine magnetite ( $\text{Fe}_2\text{O}_3$ ) was obtained by straightforward air-aqueous oxidation of standard-grade carbon steel (St3 grade). The method of preparation and properties of this kind of magnetite are described in detail in the paper [15].

Normally, EMR shielding requires protective coatings in the form of paint that can be applied to surfaces exposed to electromagnetic radiation. In that respect, liquid composites were produced using typical processes for producing paints, in which carbon materials were acting as paint fillers. Experimental samples of protective shields were prepared by the following procedure:

- (a). The filler and the polymer were carefully weighed with a Kern ABJ 220-4NM scale.
- (b). The components were mixed in certain ratios (by weight) and thoroughly stirred until they became homogeneous so that they formed a composite.
- (c). The prepared suspension was employed to obtain coatings onto a horizontal surface, as a thin layer of a certain thickness. Cardboard sheets (40 cm × 40 cm) were used as a substrate.
- (d). The composition was finally dried at room temperature.

The surface morphology of the coatings was verified by using scanning electron microscopy SEM (Jeol LV6360, Akishima, Tokyo, Japan).

The sheet resistance of conductive thin films was measured using the four-point probe system ST2558B-F01 from Suzhou Jingge Electronic Co. Jiangsu, China. Two external (polarizing) electrodes were connected to the sample and a direct current source. Two internal (measuring) electrodes were connected to a millivoltmeter with a very high internal resistance. Due to this, there was practically no current in the measuring circuit, and the contact resistance between the electrodes and the sample did not affect the measured resistance of the sample. The specific resistance was calculated by multiplying the obtained resistance by the thickness of the film and the correction factor for the four-point probe array [16].

Finally, the EMR shielding characteristics of the composite materials were investigated using a special setup, consisting of a generator, the shielding sample (shield), and a measuring device. The radiating element had a collapsible whip antenna, which was arranged vertically and parallel to the sample under investigation. The working frequency ranged from 0.3 to 4000 MHz. The intensity of EM radiation after the shield was measured with an RF Analyzer Spectran HF-4040 unit, equipped with a logarithmic periodic Aeronia HyperLOG 7040 antenna (Strickscheid, Germany). The shielding efficiency was determined as the negative logarithm of the ratio between the electromagnetic signal intensity after and before the shield, respectively. In order to measure all samples under the same conditions, an anechoic chamber was employed. Its walls were coated with the polymer-carbon material under study. Both transmitting and receiving antennas as well as the sample were placed

inside the anechoic chamber. Finally, the level of the signals without the sample between the antennas was used as the background.

### 3. Results

#### 3.1. Electrical Properties of Composites

Tables 1 and 2 present the specific resistance of two types of samples, thin coatings and pellets.

**Table 1.** Effect of carbon material and its mass concentration (weight %) on the specific resistance of dry pelleted composite material.

Conductive Additive	Mass Concentration	Specific Resistance (Ohm·cm)
Pure Black	5%	157.5
Pure Black	10%	68.3
Pure Black	15%	5.5
Pure Black	20%	0.9
CGP S-1	5%	653.2
CGP S-1	10%	0.2
CGP S-1	15%	0.1
CGP S-1	20%	0.04
CGP S-1/Pure Black	3.33%/1.67%	1314.1
CGP S-1/Pure Black	6.67%/3.33%	36.6
CGP S-1/Pure Black	8%/4%	3.9
CGP S-1/Pure Black	10%/5%	2.0
CGP S-1/Pure Black	13.33%/6.67%	0.3

**Table 2.** Specific resistance of thin composite films.

Sample ID	Concentrations of the Components (%)			Thickness (μm)	Specific Resistance (Ohm·cm)
	CGP S-1	Pure Black	Fe <sub>2</sub> O <sub>3</sub>		
1	80	-	-	60	92
2	-	80	-	60	40
3	60	20	-	60	2.4
4	60	20	-	125	1.6
5	50	17	17	60	0.8
6	50	17	17	125	0.3

The concentrations of components are given in weight percent for the solid phase. Since a polymer-carbon composite is expected to have high conductivity, depending on its composition, it is necessary to determine optimum amounts of the conductive additives within the composite that can offer the desired electrical performance. So, various polymer/conductive additive ratios were studied. The respective samples were prepared by pressing the mixture of the components under use into 12 mm-diameter pellets. The correlation between the composition and the electric resistance of the respective pellets is given in Table 1. According to these results, at 5% content of the conductive additive material, the specific resistance is fairly high. With increases in the mass fraction of the conductive additive material, the specific resistance decreased gradually. For the case of carbon-black-containing samples, a reasonable conductivity is achieved at a content of about 15%. For the case of thermally expanded graphite, a reasonable conductivity was

achieved at a 10% content of the additive. In samples containing the mixture of conductive additives (graphite and carbon black), the conductivity was found to decrease to some extent. When the mass fraction of conductive additives was increased to 20%, a relatively small increase was observed in conductivity, a fact indicating that the percolation threshold was reached at this content [17,18]. The observed results are consistent with the percolation theory. Considering the assumptions of the percolation theory, the threshold of conductivity change can be calculated as follows:

$$\sigma = \sigma_0(x - x_c)^t \quad (1)$$

where  $\sigma_0$  is the conductivity at 100% concentration of the conducting phase (at  $x = 1$ );  $x_c$  is the limiting concentration, which corresponds to the percolation threshold;  $t$  is the limiting index of conductivity. For a two-dimensional system,  $x_c = 0.5$ , whereas for a three-dimensional system,  $x_c = 0.16$  [19,20]. Based on Equation (1) and experimental Tables 1 and 2, it can be observed that the content of the carbon additive in the proposed paints significantly exceeds the theoretical percolation threshold. For the goal of this work, namely to obtain EMI shielding effective paints, it is important only to be above the percolation threshold. The exact location of the threshold is not relevant for this case. Using the model for a clearer approximation would not add any value to this work, nor valuable information for scientific purposes, since, for carbon materials, these data are strongly connected to the kind of used carbon allotrope and its provider-related particular properties.

Although mass concentrations of fillers given in Table 2 are higher than the percolation threshold, the coatings containing graphite and carbon black show a considerable resistance, those based on graphite exhibiting the highest one. On the other hand, according to Table 1, the graphite-based polymer composites pellets possess a better conductivity. Moreover, it is observed that the conductivity increases considerably when a mixture of conductive additives is used. Regarding the addition of magnetite, this also improves the conductivity. Finally, the increase in thickness of the coatings leads to a decrease in the specific resistance.

Following the previous results, it seems that a sharp change in the morphology and roughness of contour probably occurs when using the mixture of conductive additives and magnetite. Additionally, the uniform distribution of the carbon particles in the bulk of the sample should be taken into account, as well as the process of particles merging into large agglomerates. If the size of agglomerates formed is comparable with the thickness of the layer, they can be located in one direction, which means that the three-dimensional system changes to the two-dimensional one [21]. Consequently, the conductivity of systems containing only the carbon filler is likely to exhibit worse performance according to Equation (1). Thus, the minimum conductivity observed for the graphite (Table 2), even at a concentration of about 80% in the solid phase, might be due to the change from a three-dimensional system to a two-dimensional one, i.e., the formation of agglomerates in the layer of coating, with their average size reaching the thickness of the layer (in terms of the order of magnitude). The addition of magnetite probably affects the breakdown of the agglomerates. So, high conductivity is observed for samples 5 and 6 (Table 2) even at a lower content of carbon filler.

Scanning Electron Microscopy (SEM) was used to understand the structuring of the coatings and particularly the influence of the presence of the nanofillers within the structure and film morphology. Figure 1 shows SEM images of the samples with various carbon materials at two different magnifications.

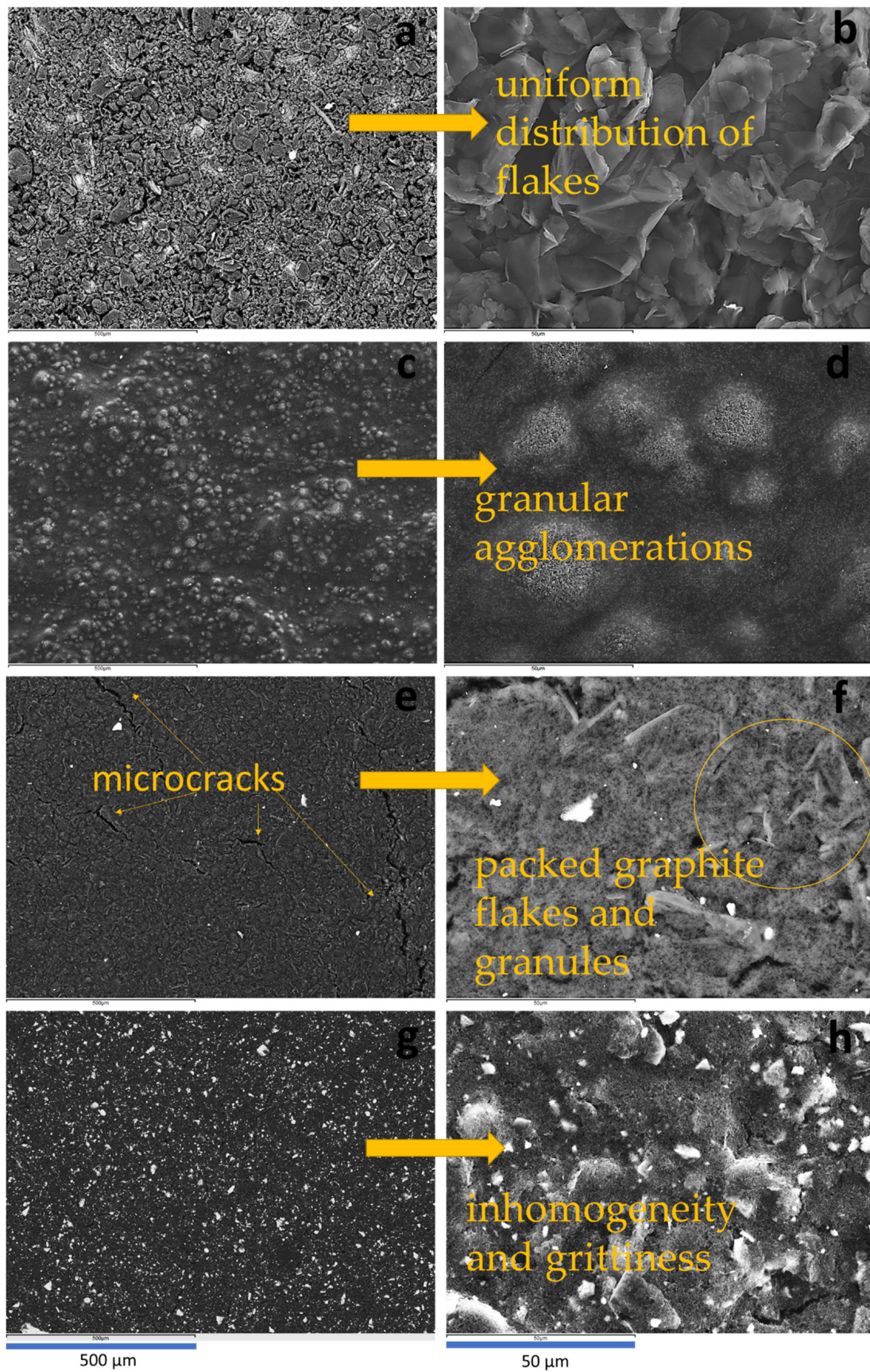


**Figure 1.** SEM images of the composite films at different magnification (listed in Table 2): (a,b) Sample #1, (c,d) Sample #2, (e,f) Sample #3, (g,h) Sample #5.

As can be observed in the SEM images in Figure 1, the use of different conductive fillers and their combination can lead to different structurings of coatings based on the composite materials. Figure 1a,c,e,g represent a general view of the surface of composites containing graphite (Figure 1a), PUREBLACK (Figure 1c), their combination (Figure 1e), and their combination with the addition of  $\text{Fe}_2\text{O}_3$ , respectively (Figure 1g), all at smaller magnification. It is obvious that the conductive filler plays a very important role in structuring the layers of the composite material. The presence of graphite can be associated with the uniform distribution of flakes, while the use of PUREBLACK leads to granular agglomerations, which are also distributed along the surface of the coating. The combination of these two conductive fillers leads to a more compact coating consisting of packed graphite flakes and granules. The addition of  $\text{Fe}_2\text{O}_3$  in the composite seems to increase the surface inhomogeneity and grittiness. Moreover, in the images of Figure 1b,d,f,h, at the higher magnification, it can be observed that the presence of graphite seems to promote microcrack formation (Figure 1a) that become more prevalent and larger in the mixed formulation (Figure 1e). The structuring and morphology of the coatings observed by SEM support the specific resistance variation as a function of the filler nature described above.

### 3.2. Shielding Properties of Composites

Polymer composites containing carbon materials present significant interest since they are natural products that can be employed for the absorption of ultra-high frequency (UHF) radiation. These UHF absorption properties were studied for the developed samples and presented in Table 2 so that these can be compared in order to obtain the composition of optimum shielding performance. To measure the absorption parameters, the technique described in [22,23] was used. The study of the EMR shielding characteristics of the composite layers was carried out with the special setup shown in Figure 2, which enables quick and efficient evaluation of EMR shielding properties of coatings in the 300 MHz–4 GHz frequency range.

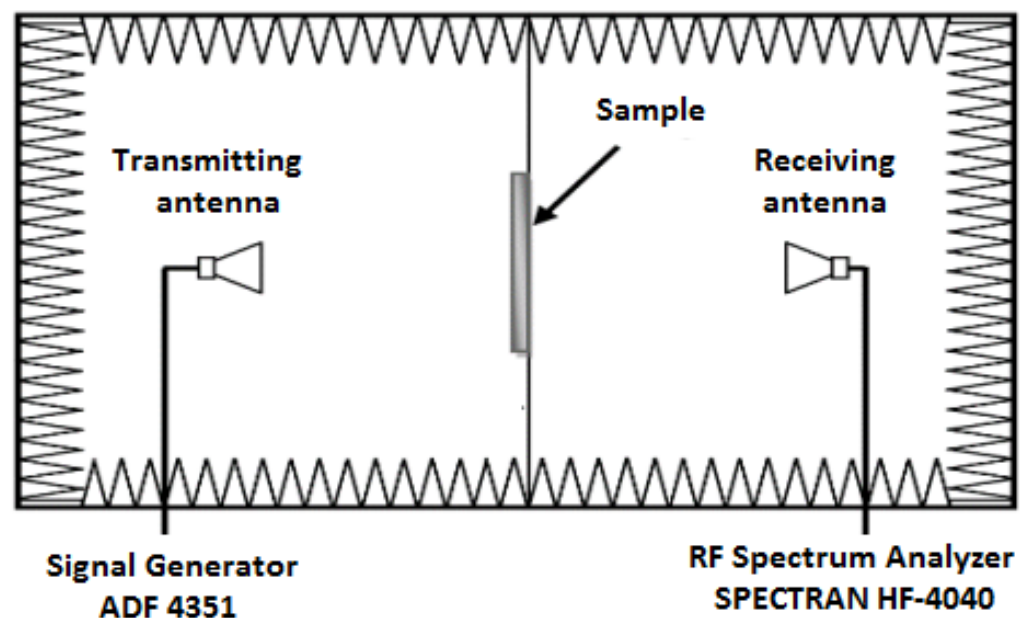
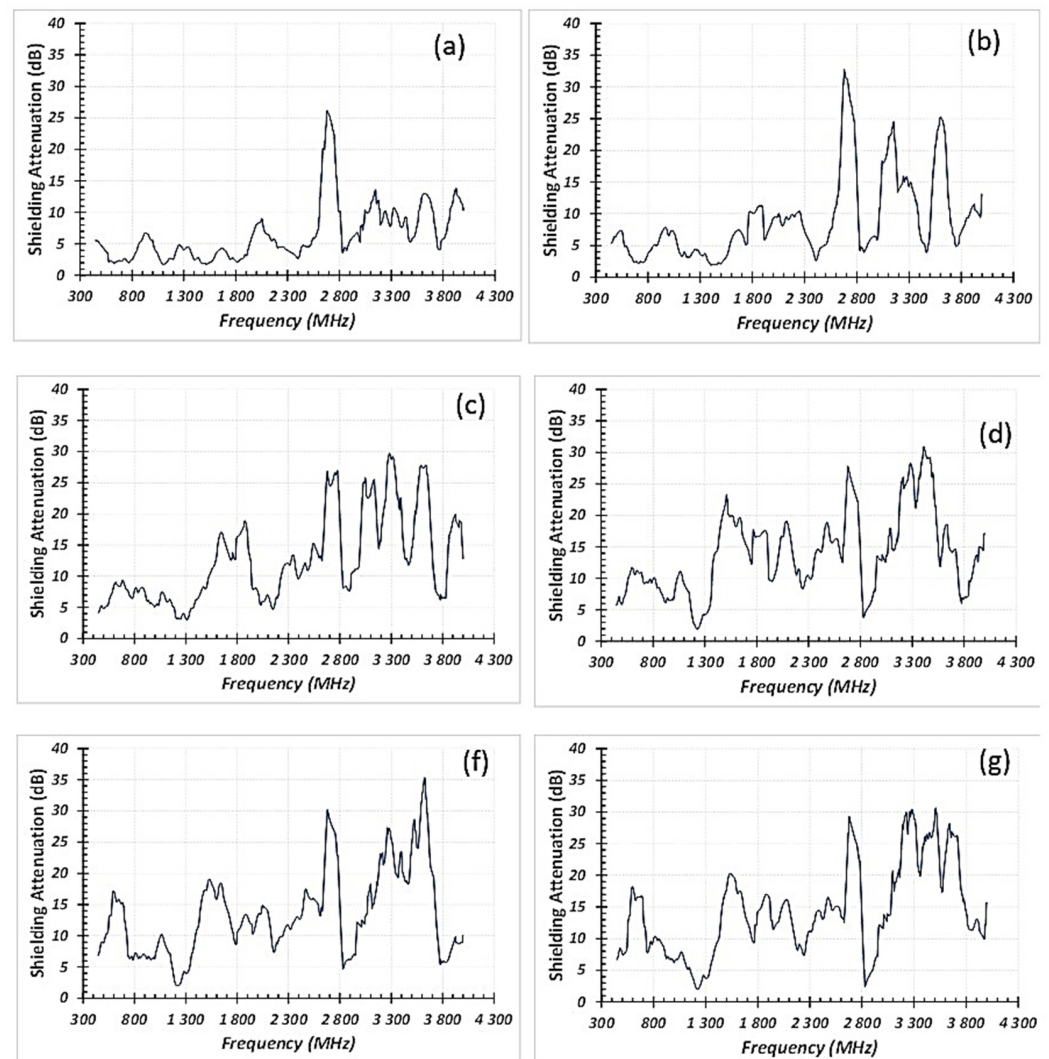


Figure 2. Transmission technique for measuring electromagnetic shielding in anechoic chamber.

Figure 3 shows results for SA of the composite films. As can be seen, SA is increasing for all samples with increasing frequency. The results shown in Table 3 indicate that the SA of the polymer-carbon composites under study is from  $-10$  dB to  $-30$  dB, even though no additional magnetic components were introduced to the composites. Understanding that this effect is achieved at the contact boundary of the components of the polymer-carbon composites can help in developing new EMR protective coatings. The optimization of the

composites by adding magnetite was found to increase the shielding performance. This is an effect that correlates well with the conductivity of the composite materials (Table 2). Therefore, as expected, the composition and the morphology of the composite films affect their shielding efficiency parameters. To find a correlation of the shielding properties with the microstructure, thickness, and composition of the paint-like materials and the respective coatings, further studies are ongoing. The shielding mechanism for multicomponent composite materials is not yet clear enough and, in the case of our composites, assumptions on the mechanism would be only speculative. Based on SEM observations and specific resistance values, one can assume that the coherent multiple reflections at the internal interfaces may contribute to an increase in the shielding efficiency. PVB seems to be just linking the fillers without affecting the shielding performance of the composite material. The results revealed that composites with magnetite seem to provide enhanced absorption shielding performance. Composites filled with carbon black are not able to efficiently absorb electromagnetic radiation in the given frequency range, while the graphite-containing composites are more effective. Finally, the combination of carbon black and graphite resulted in the modification of both morphological characteristics of the coating and their absorption shielding ability.



**Figure 3.** Shielding attenuation for frequency range from 300 MHz to 4000 MHz for coatings with different thickness and composition (listed in Table 2): (a) Sample #1; (b) Sample #2; (c) Sample #3; (d) Sample #4; (e) Sample #5; (f) Sample #5; (g) Sample #6.

**Table 3.** Frequency dependence of the shielding attenuation of films based on different carbon materials.

Sample ID	Average Shielding Attenuation (SA), dB				SA Maximum/ Corresponding Frequency (dB/GHz)
	Frequency Range: 0.3–1.0 GHz	Frequency Range: 1.0–2.0 GHz	Frequency Range: 2.0–3.0 GHz	Frequency Range: 3.0–4.0 GHz	
1	4.1	3.7	7.8	9.8	26/2.70
2	4.9	6.0	10.1	14.1	32/2.69
3	6.6	9.7	13.2	18.6	30/3.30
4	8.4	13.2	14.3	18.5	32/3.40
5	9.1	11.6	13.7	17.8	35/3.7
6	9.8	11.6	13.5	21.3	31/3.3 (3.6)

The values of SA were found to range from 9.1 dB to 17.8 dB for samples with a 60  $\mu\text{m}$  thickness, the effectiveness increasing from 9.1 dB to 21.3 dB for doubled thickness. Therefore, the film thickness seriously affects the shielding effectiveness. This result is similar to that reported by other teams using more expensive conductive fillers, such as an EMI shielding paint based on reduced graphene oxide (rGO) conjugated with ferromagnetic nanostructures. An absorption of up to about 12 dB has been reported for a composite based on rGO-Fe<sub>3</sub>O<sub>4</sub> and about 18 dB for a composite of rGO-Ni [24]. Moreover, a graphene/Fe<sub>3</sub>O<sub>4</sub> composite has been reported to present good electromagnetic shielding performance.

It can be concluded that these protective films, based on a mixture of carbon materials, possess high conductivity at high frequencies, which, in turn, improves the shielding effectiveness.

#### 4. Conclusions

Paint-like composites based on mixtures of carbon materials with magnetite were developed, applied as layers by painting, and their EMR shielding performance was studied. It was found that in order to achieve high EMR shielding effectiveness, it is necessary not only to have a quite high content of carbon components in the composite, but also to avoid the agglomeration of filler particles. Using these paint-like materials with carbon fillers, coatings absorbing UHF radiation with a shielding effectiveness of up to  $-35$  dB can be obtained. The material possesses a minimum reflection coefficient as it does not contain any metallic substance. The materials proposed can be used to provide the electromagnetic compatibility of radio-electronic devices as well as the electromagnetic shielding of living beings against microwave radiation.

**Author Contributions:** Conceptualization, V.K. and V.B.; Data curation, O.B. and O.C.; formal analysis, V.K., V.B., M.P.S. and E.K.; funding acquisition, V.B. and E.K.; investigation, V.K., O.B. and O.C.; methodology, V.B., V.K. and E.K.; project administration, V.B. and E.K.; validation, V.K., V.B., M.P.S. and E.K.; visualization, O.B. and O.C.; writing—original draft, V.K., V.B., M.P.S. and E.K.; writing—review and editing, M.P.S. and E.K. All authors have read and agreed to the published version of the manuscript.

**Funding:** This research was funded in part by the NATO Science for Peace and Security Programme under grant G5477. The APC was funded by MPS (personal mdpi vouchers).

**Institutional Review Board Statement:** Not applicable.

**Informed Consent Statement:** Not applicable.

**Data Availability Statement:** The raw and processed data required to reproduce these findings cannot be shared at this time due to technical or time limitations. The raw and processed data will be provided upon reasonable request to anyone interested anytime until the technical problems will be solved.

**Acknowledgments:** IMT contribution was partially financed by the Romanian Ministry of Research, Innovation and Digitization through “MICRO-NANO-SIS PLUS” Programme.



**Conflicts of Interest:** The authors declare no conflict of interest. The funders had no role in the design of the study; in the collection, analyses, or interpretation of data; in the writing of the manuscript, or in the decision to publish the results.

## References

1. Pawar, S.P.; Biswas, S.; Kar, G.P.; Bose, S. High Frequency Millimetre Wave Absorbers Derived from Polymeric Nanocomposites. *Polymer* **2016**, *84*, 398–419. [CrossRef]
2. Cekan, P.; Hovanec, M.; Sabo, J. Human factor in conversation between subordinates and managers. *Nase More* **2016**, *63*, 241–243. [CrossRef]
3. Barnes, F.S.; Greenebaum, B. (Eds.) *Biological and Medical Aspects of Electromagnetic Fields*, 3rd ed.; CRC Press: Boca Raton, FL, USA, 2018.
4. Krewski, D.; Byus, C.V.; Glickman, B.W.; Lotz, W.G.; Mandeville, R.; Salem, T.; Weaver, D.F. Recent advances in research on radiofrequency fields and health: 2001–2003. *J. Toxicol. Environ. Health* **2001**, *4*, 145–159. [CrossRef] [PubMed]
5. Stilgoe, J. The (co-)production of public uncertainty: UK scientific advice on mobile phone health risks. *Public Underst. Sci.* **2007**, *16*, 45–61. [CrossRef]
6. Hardell, L.; Mild, K.H.; Carlberg, M. Further aspects on cellular and cordless telephones and brain tumours. *Int. J. Oncol.* **2003**, *22*, 399–407. [CrossRef]
7. Aerts, S.; Plets, D.; Verloock, L.; Martens, L.; Joseph, W. Assessment and comparison of total RF-EMF exposure in femtocell and macrocell base station scenarios. *Radiat. Prot. Dosim.* **2014**, *162*, 236–243. [CrossRef]
8. Ott, H.W. *Electromagnetic Compatibility Engineering*; Wiley: New York, NY, USA, 2009.
9. Wake, K.; Laakso, I.; Hirata, A.; Chakarothai, J.; Onishi, T.; Watanabe, S.; de Santis, V.; Feliziani, M.; Taki, M. Derivation of Coupling Factors for Different Wireless Power Transfer Systems: Inter- and Intralaboratory Comparison. *IEEE Trans. Electromagn. Compat.* **2016**, *59*, 677–685. [CrossRef]
10. De Paulis, F.; Nisanci, M.H.; Orlandi, A.; Koledintseva, M.Y.; Drewniak, J.L. Design of Homogeneous and Composite Materials from Shielding Effectiveness Specifications. *IEEE Trans. Electromagn. Compat.* **2014**, *56*, 343–351. [CrossRef]
11. Mirotznik, M.S.; Yarlagadda, S.; McCauley, R.; Pa, P. Broadband electromagnetic modeling of woven fabric composites. *IEEE Trans. Microw. Theory Technol.* **2012**, *60*, 158–169. [CrossRef]
12. De Rosa, I.M.; Mancinelli, R.; Sarasini, F.; Sarto, M.S.; Tamburrano, A. Electromagnetic Design and Realization of Innovative Fiber-Reinforced Broad-Band Absorbing Screens. *IEEE Trans. Electromagn. Compat.* **2009**, *51*, 700–707. [CrossRef]
13. Wang, X. Investigation of Electromagnetic Shielding Effectiveness of Nanostructural Carbon Black/ABS Composites. *J. Electro-magn. Anal. Appl.* **2011**, *3*, 160–164. [CrossRef]
14. Mikinka, E.; Siwak, M. Recent advances in electromagnetic interference shielding properties of carbon-fibre-reinforced polymer composites—A topical review. *J. Mater. Sci. Mater. Electron.* **2021**, *32*, 24585–24643. [CrossRef]
15. Butenko, O.; Boychuk, V.; Savchenko, B.; Kotsyubynsky, V.; Khomenko, V.; Barsukov, V. Pure ultrafine magnetite from carbon steel wastes. *Mater. Today Proc.* **2019**, *6*, 270–278. [CrossRef]
16. Ramadan, A.A.; Gould, R.D.; Ashhour, A. On the Van der Pauw method of resistivity measurements. *Thin Solid Films* **1994**, *239*, 272–275. [CrossRef]
17. Kruželák, J.; Kvasničáková, A.; Hložeková, K.; Hudec, I. Progress in polymers and polymer composites used as efficient materials for EMI shielding. *Nanoscale Adv.* **2021**, *3*, 123–172. [CrossRef]
18. Rahaman, M.; Chaki, T.K.; Khastgir, D.J. Development of high performance EMI shielding material from EVA, NBR, and their blends: Effect of carbon black structure. *J. Mater. Sci.* **2011**, *46*, 3989–3999. [CrossRef]
19. Brigandi, P.J.; Cogen, J.M.; Pearson, R.A. Electrically conductive multiphase polymer blend carbon-based composites. *Polym. Eng. Sci.* **2014**, *54*, 1–16. [CrossRef]
20. Tiwari, J.N.; Tiwari, R.N.; Kim, K.S. Zero-dimensional, one-dimensional, two-dimensional and three-dimensional nanostructured materials for advanced electrochemical energy devices. *Prog. Mater. Sci.* **2012**, *57*, 724–803. [CrossRef]
21. Morari, C.; Balan, I. Methods for determining shielding effectiveness of materials. *EEA* **2015**, *63*, 126–136.
22. Galehdar, A.; Rowe, W.; Ghorbani, K.; Callus, P.J.; John, S.; Wang, C.H. The effect of ply orientation on the performance of antennas in or on carbon fibre composites. *Prog. Electromagn. Res.* **2011**, *116*, 123–136. [CrossRef]
23. Parmar, S.; Ray, B.; Date, K.; Datar, S. Modified graphene as a conducting ink for electromagnetic interference shielding. *J. Phys. D Appl. Phys.* **2019**, *52*, 375302. Available online: <https://iopscience.iop.org/article/10.1088/1361-6463/ab2abb/pdf> (accessed on 1 April 2022). [CrossRef]
24. Li, L.; Yanjun, C.; Zhixia, Z.; Peng, T.; Haipeng, G.; Ping, L. Preparation of graphene/Fe<sub>3</sub>O<sub>4</sub> composite varnish with excellent corrosion-resistant and electromagnetic shielding properties. *Ceram. Int.* **2020**, *46*, 22876–22882. [CrossRef]